JOURNAL OF ENGINEERING annals OF FACULTY OF ENGINEERING HUNEDOARA
TOME VI (year 2008), FASCICULE 2, (ISSN 1584 – 2665)

STUDY OF INJECTION PARAMETERS ON PERFORMANCE AND FUEL CONSUMPTION IN A PORT-INJECTED GASOLINE ENGINE WITH EXPERIMENTAL AND THEORETICAL METHODS

F. OMMI[1], E. MOVAHEDNEJAD[2], K. NEKOFAR[3]

[1, 2]FACULTY OF ENGINEERING, TARBIAT MODARES UNIVERSITY, TEHRAN, IRAN
[3]IRANIAN SPACE AGENCY, TEHRAN, IRAN

ABSTRACT:
For spark ignition engines, the fuel-air mixture preparation process is known to have a significant influence on engine performance and exhaust emissions. The structures of port injector spray dominates the mixture preparation process and strongly affect the subsequent engine combustion characteristics over a wide range of operating conditions in port-injection gasoline engines. In this paper, a one-dimensional, unsteady, multiphase flow has been modeled to study the mixture formation process in the intake manifold for a port-injected gasoline engine. Also, an experimental study is made to characterize the breakup mechanism and spray characteristics of a conventional Multi-hole injector used in the engine. The distributions of the droplet size and velocity and volume flux were characterized by a PDA system. One dimensional air flow and wall fuel film flow and a two dimensional fuel droplet flow have been modeled and it includes the effects of in-cylinder mixture back flows into the port. As a result, predictions are obtained that provide detailed picture of the air-fuel mixture properties along the intake port. A comparison was made on injection characteristics of the multi-hole injectors and its effects on multi-phase flow property on various fuel pressures and temperatures. According to the present investigation, it was found that the injector produces a finer spray with a wide spray angle in higher fuel pressures and temperatures which refine fuel-air mixture characteristics in intake port. Higher values of fuel temperature also produce optimum conditions for both exhaust emission and performance.
KEYWORDS:
exhaust emission, PDA system, gasoline engine

1. INTRODUCTION

The desire for increased fuel economy in conjunction with stringent emission regulations has nowadays, forced the automotive industry to make substantial changes in the design and operation of gasoline engines. Mixture preparation precedes all the other engine processes by metering the ambient air and fuel and forming a mixture that satisfies the requirements of the engine over its entire operating regime, and as a result, has a dominant effect on the subsequent combustion process and control the engine fuel consumption, power output, exhaust emissions and other operating performance. The mixture formation process in current automotive gasoline engines begins with liquid fuel being introduced into the intake port and simultaneously metered by gasoline port injector. It is followed by a simultaneous transfer of heat, mass and momentum between a highly turbulent and pulsating air flow and liquid fuel spray in a confined space. Fuel droplets exit with an average size, velocity and different trajectories, which determine spray targeting performance. All these spray characteristics are determined by particular injector design and operating

conditions [1]. Many spray parameters including fuel metering, atomization characteristics, targeting, and pulse-to-pulse variability have a direct impact on engine performance [2]. An optimized spatial fuel distribution plays a key role in reducing fuel wall attachment and thus, improving engine transient response and reducing hydrocarbon (HC) emissions, which is greatly determined by injector design and intake port geometry. A better understanding of spray characteristics of port injector is very important in matching spray parameters with different engine operations. As a result, there is an explosive increase of research publications in port injector sprays [3-7]. Senda et al. [8, 9] investigated the spray atomization mechanism at different back pressures, namely ambient pressure. It was found that when the liquid fuel is injected into the ambient with a back pressure below that of the equilibrium pressure, i.e., the saturated vapor pressure, the atomization process is enhanced markedly due to flash boiling vaporization phenomena.

Quan Zhao (1995) reported a study of the spray breakup of a regular and an air-shrouding injector and the global spray structures from these two types of port injectors were visualized under steady and transient conditions over different fuel injection pressures. The results showed the importance of agreement between spray characteristics and engine parameters [1].

Over the years, there have been a number of investigations concerning the mixture preparation processes in both carbureted and fuel-injected spark-ignition engines with a one-dimensional approach. However, most of the previous studies either neglected the interactions between droplet vaporization, liquid film flow gas-and liquid-phase temperature and species change, or neglected the transient or neglected the liquid film flow on the wall. Gang Chen (1996) developed a one dimensional, unsteady, multi component, multiphase flow to study the mixture formation process in the intake manifold for a port-injected gasoline engine [10].

This paper reports an experimental study of the spray breakup and injection characteristics of a regular Multi-hole port fuel injector for applications to 8-valve Multi-point fuel injection engines. The global spray structure from this injector was measured under steady conditions over different fuel injection pressures and fuel temperatures and characterized using phase Doppler anemometry (PDA) technique. Also, a model of a 4 cylinder multi-point fuel injection engine (XU7JP-L3) was prepared using a fluid dynamic code (WAVE) from intake air to throttle body to exhaust gas from muffler. By this code one-dimensional, unsteady, multiphase flow in the intake port has been modeled to study the mixture formation process in port including the effects of in-cylinder mixture back flow into the port and to determine the effect of fuel pressure and temperature on mixture properties. The model consists of three major parts: a gas-phase model, liquid-film model and fuel droplets model. One dimensional air flow and wall fuel film flow models and a two dimensional fuel droplet flow model have been developed. As a result, predictions are obtained that provide detailed picture of the air-fuel mixture properties along the intake port. The model identifies the effects of each parameter, like fuel pressure and fuel temperature on the final mixture and shows the interactive influences of three phases of the mixture during the process. The model helps to understand the behavior of multiphase flow in the intake port, and can give guidelines toward achieving more efficient, clean and smooth engine operation.

2 EXPERIMENTAL TECHNIQUES

The experimental technique used in this work is a laser base technique. To obtain the detailed quantitative information of the sprays, a two-component Phase Doppler Anemometry (PDA) was used to perform the simultaneous measurements of the droplet velocity and size and the volume flux. The injector is side-feed and it is placed in a quiet sealed cylinder that cans feeds the injector through it's around.

The measurement locations were set at outlet nozzle, 100 mm downstream as far as the targeting point of the spray is located 00 mm downstream of intake valve. In the present study, the measurement is being done for maximum 1500 droplets in time duration of 15 seconds.

This ensured repeatable results for spray characteristics. Water was used to feed the injector for visualizing the spray breakup and atomization process. The fuel injection pressure and fuel temperature were changed in the range of 200 to 500 (200, 300, 400, and 500) Kpa and in the range of 25 to 70C; respectively. Considering difference between physical properties of water and gasoline, correction factors were used to convert the measured results for water to gasoline.

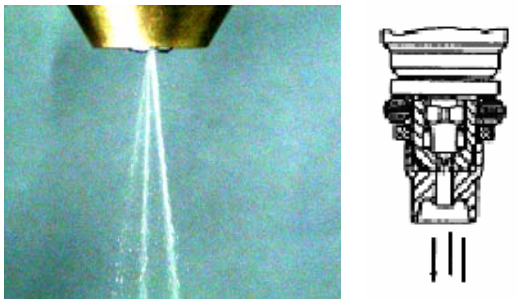

Fig. 1: a) injector nozzle geometry (right)
b) Spray pattern in injector model (left)

The injector model is a conventional Ball-valve Multi-hole injector with three jets in exit. Figure 1 shows the visualization results of the spray caused by a multi-hole baseline compound injector which has three square exit metering holes for producing three spray jets. In this injector once the valve opens, the main flow of fuel passes nozzle and impinge on a plate with three holes and separates into three jets.

Droplet vertical velocity distribution at 100 mm downstream, for P = 300 Kpa and T = 250 C, is shown in figure 2. There are three high velocity zones that represent three separate jets in spray pattern as it is seen in figure 1. The average value of more powerful jet is about two times of weaker ones.

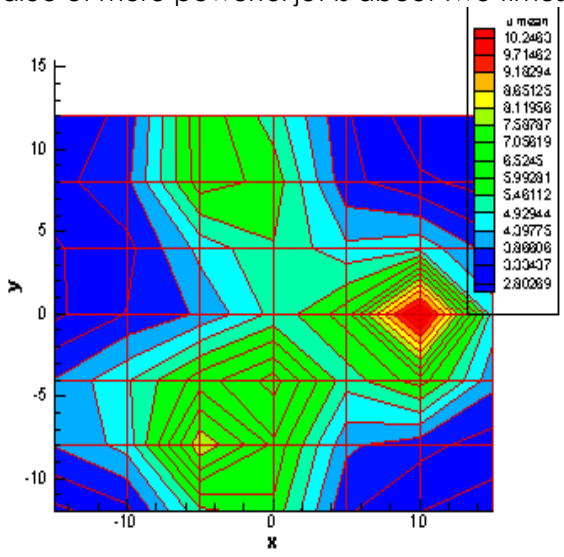

Fig. 2: Distribution of droplets velocity (m/s) in 100 mm downstream and 300 Kpa, 25 C

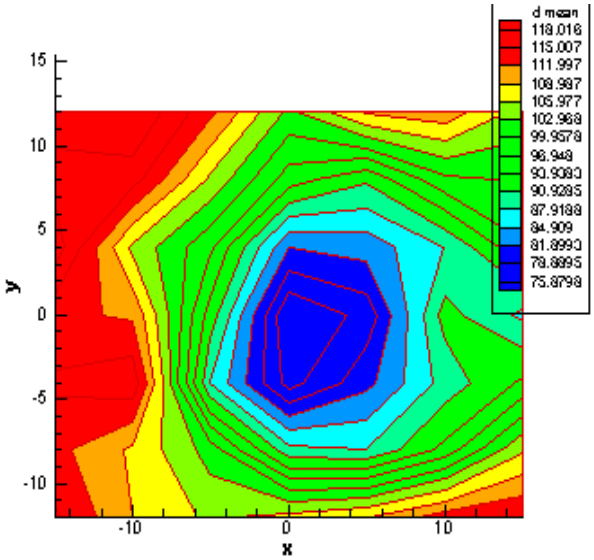

Fig. 3: Mean diameter distribution of droplets (micron) in 100 mm downstream and 300 Kpa, 25 C

Figure 3 shows mean diameter distribution of droplets in micron. According this figure, droplets with leas mean diameter are placed in center of spray cone and the diameter increases along radius. The frequency diagram of droplets diameter is shown in Figure 4.

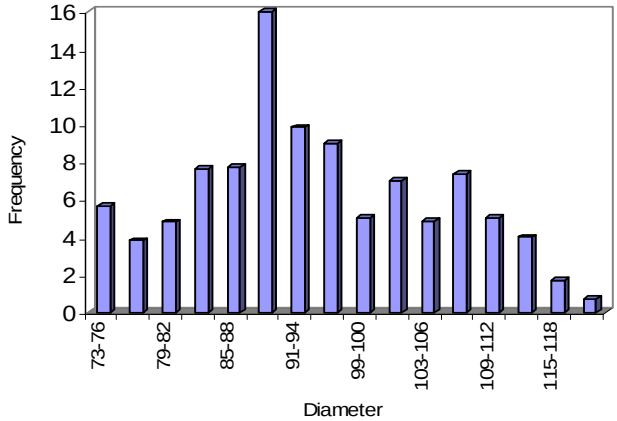

Fig. 4: Frequency diagram of droplets mean diameter

Table 1: Injection characteristics in various fuel pressure for 25 c

Fuel pressure (kpa)	200	300	400	500
Initial mean velocity (m/s)	11.9	13.1	14	16.1
Sautre Mean diameter (micron)	81	77	74.3	71.5
Injection rate (kg/hr)	6.99	8.39	9.9	11.3
Spray cone angle	11	15	20	24

Table 2: Injection characteristics in various fuel temperatures for fuel pressure 3 bar

Fuel temperature (c)	25	40	50	60
Initial mean velocity (m/s)	13.2	14.3	16.7	21.6

The injection parameters e.g. the mean diameter (SMD), the velocity and spray cone angle in different pressure and temperature are to be specified since they are required for the modeling of injection and vaporization. These results are shown for different fuel pressures and fuel temperatures for nozzle outlet in table 1 and 2 respectively.

3. PHYSICAL MODELS

After injection, the droplets flow takes place in the intake port whose geometry is shown in figure 5.

As the droplet group moves in the hot gas stream, it decelerates or accelerates depending on operating conditions. At the same time, the droplets vaporization is initiated. As the droplets move to the end of the pipe, some of the unvaporized droplets are assumed to impinge on the intake port wall bend to form a droplet deposition flux. Because of the heat transfer from the wall and from the air stream, the liquid film continuously vaporizes. The processes described above influence the state of the gas, i.e., the gas stream may be retarded, speeded up, cooled and enriched with fuel-vapor components. The changes in the gas-phase properties in turn influence the dynamics and vaporization of droplets, which are subsequently injected [10].

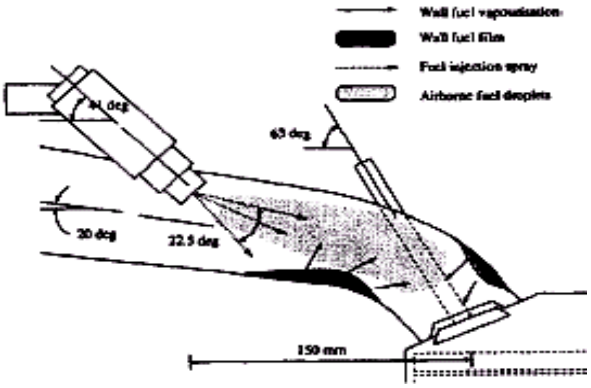

Fig. 5: Intake port geometry

Wave is a computer-aided code to analyze the dynamic of pressure waves, mass flows and energy loses in various systems and machines. It provides a fully integrated treatment of time-dependent fluid dynamics and thermodynamics by means of one dimension formulation.

The basic engine model is a time-dependent simulation of in-cylinder processes, based upon the solution of equations for mass and energy according two-zone combustion model in which the cylinder is divided to two regions: unburned zone and burned zone which share a common pressure.

The mass equation accounts for changes in cylinder mass due to flow through valves and due to fuel injection. A separate accounting is made for fluxes of air, vaporized fuel, liquid fuel and products of combustion. The liquid fuel is assumed to have mass but to occupy only a very small volume (very high density compared to the gases).

The energy equation is based on the first law of thermodynamics and equates the change of internal energy of in-cylinder gases to the sum of enthalpy fluxes in and out of the chamber, heat transfer and piston work.

For the unburned zone in the 2-zone description, equation for energy is:

$$m_{u1}U_{u1}-m_{u0}U_{u0}+m_{u1}R_{u1}-PV_{u0}+Q_u-\Delta m_{ui}h_{ui}=0 \quad (1)$$

Similarly, for the burned it is:

$$m_{b1}U_{b1}-m_{b0}U_{b0}+m_{b1}R_{b1}T_{b1}-PV_{b0}+Q_b+\Delta m_{bi}h_{bi}=0 \quad (2)$$

Under a constraint condition, the volumes of the unburned and burned zones are summed up to the total cylinder volume:

$$m_{u1}R_{u1}T_{u1}+m_{b1}R_{b1}T_{b1}-PV_C=0 \quad (3)$$

The last three equations are a complete set and are solved by using the Newton iteration method.

3.1. Fuel injection

This code anticipates spray distribution, droplet evaporation and formation and transport of fuel film along intake port using various injector models and governing equation of transport and evaporation of droplets. WAVE contains two different liquid fuel evaporation models: an in-cylinder only model and a comprehensive fuel spray evaporation model, which predicts liquid evaporation through the entire flow network. The first general fuel spray model predicts fuel evaporation in engine cylinders only. This model allows liquid fuel to evaporate up to the saturation vapor pressure, at which the evaporation will halt. If conditions in the cylinder change so the saturation vapor pressure is reduced below the current vapor pressure of fuel in the cylinder, fuel will condense back into liquid form. The rate of evaporation of liquid fuel is calculated by first determining the fuel mean drop diameter (SMD) and characteristic evaporation time τ_{eva} according below equation:

$$\frac{dm_v}{dt} = (m_l - m_v) \Big/ \tau_{eva} \tag{4}$$

where m_l is the liquid fuel and m_v is the mass of the fuel vapor. τ_{eva} is time factor calculated based on the energy balance between the surrounding air and the liquid fuel and the assumption that the heat transferred is a fraction of the available energy.

3.2. Comprehensive fuel spray model

The comprehensive fuel spray model predicts liquid fuel spray motion and evaporation. It also includes a more detailed treatment of in-cylinder evaporation. From the measurements by Hiroyasu, Arai and Tabata (1989), for low-pressure injectors, the Sauter mean diameter d_{32} can be correlated as [3]:

$$SMD = 4.12 d_{nozz} Re^{0.12} We^{-0.75} \left(\frac{\mu_f}{\mu_g}\right)^{0.54} \left(\frac{\rho_f}{\rho_g}\right)^{0.18} \tag{5}$$

where d_{nozz} is the nozzle diameter, μ_f and μ_g the fuel and gas dynamic viscosity, respectively, Re the Reynolds number and We the Weber number.

It assumes that the droplets in the spray have a non-uniform size distribution in a function suggested by Rosin & Rammler (1933).

3.3. Droplet dynamics

During the spray penetration, there is a drag force exerted on the droplets from the surrounding gases, which tends to decrease the relative velocity between the drop and the gas flow. From the Newton's Second Law (Bird et. al. 2002), the equation is:

$$m_f \frac{du_f}{dt} = \frac{1}{2} C_D \rho_g |u_g - u_f| (u_g - u_f) \frac{\pi d^2}{4} \tag{6}$$

Where d is the droplet diameter, u_g and u_f are the velocities of the gas flow and the liquid fuel droplet, respectively. And the drag coefficient C_D is given by Choi and Lee (1992), as below:

$$C_D = 2.3 Re^{-0.37} \tag{7}$$

3.4. Droplet evaporation

The droplet evaporation rate is given by Bird (2002):

$$\omega = \frac{\rho D_{AB}}{d} sh^* \ln(1 + B_m) \tag{8}$$

where d is the droplet diameter, D_{AB} the gas diffusivity, Sh* the non-dimensional Sherwood number, and B_m the mass transfer number. The mass transfer number B_M is equal to:

$$B_M = \frac{Y_{fs} - Y_{f\infty}}{1 - Y_{fs}} \tag{9}$$

where Y_{fs} and $Y_{f\infty}$ are the mass fractions of fuel vapor at the droplet surface and the ambient, respectively.

The heat flux available for heating up the droplet is:

$$m_f \frac{c_{pf}}{\pi d^2} \frac{d(T_m)}{dt} = \omega \left[\frac{\xi c_{p\infty} (T_\infty - T_S)}{B_M} - L_v \right] \tag{10}$$

where T_∞ the ambient temperature, and ξ the correction factor to account for the effect of evaporation on heat transfer. (Abramzon and Sirignano, 1989)

The gas phase temperature is evaluated from the one-third rule (see Yuen and Chen 1976):

$$T_G = T_S + (T_\infty - T_S)/3 \tag{11}$$

3.5. Spray wall impingement

In an engine system, a liquid fuel spray may impinge on the solid walls, either on the smooth sidewalls in ducts, manifolds and cylinders. The program itself can find the impingement site, and with the given fuel spray cone angle and impingement incidence angle, it can estimates the nominal area covered by the spray cone angle from the duct geometry.

For each impingement site, the impingement probability and the passing-by probability then are assumed to be proportional to the spray covered wall area and the downstream flow cross-sectional area. The droplets in the cylinder can be discharged to the exhaust duct, when the exhaust valve opens. It is assumed that the droplets are uniformly distributed within the cylinder.

There exists a wide range of spray wall impingement regimes, which have been identified as, Adhesion, Rebound, Spread and Splash. The outcomes of impingement depend on the incoming droplet conditions: droplet velocity, size and temperature, incidence angle, wall temperature, surface roughness, wall film thickness and fluid properties, such as viscosity and surface tension.

3.6. Film dynamics

There are two different forces exerted on a fuel wall film. On the gas side, the gas flow tends to drive the film moving along the same direction. On the wall side, the viscous friction tends to resist the film movement. The force balance on the film gives the equation for the film motion:

$$\begin{aligned} \rho_f \delta \frac{du_{fm}}{dt} &= \tau_g - \tau_w + \tau_{imp} \\ \tau_g &= \frac{1}{2} f \rho_g (u_g - u_{fs}) |u_g - u_{fs}| \\ \tau_w &= 2\mu_f \frac{u_{fm}}{\delta} \qquad \tau_{imp} = \frac{\sum m_p U_t}{A \Delta t} \end{aligned} \tag{12}$$

In this equation, τ_g, τ_w and τ_{imp} are the driving force on the gas side, the viscous stress On the wall side and the momentum source per unit film area due to the impingement respectively. (Bird et. al. 2002)

Where u_{fs} is the film surface velocity and the friction factor ρ is a function of the gas flow Reynolds number. μ_f, u_{fm} and δ are the fuel dynamic viscosity, the mean film velocity, and the film thickness respectively. Also m_p is the mass converting into the film within a given sub volume during a time interval, and U_t the tangential component of droplet velocity.

3.7. Film evaporation

The film vaporization rate is determined by (see Bird et. al. 2002)

$$\omega = h_D B_M$$

where h_D is the mass transfer coefficient, and B_M the mass transfer number, as described above. For the wall film, the energy equation is described by:

$$\rho_f c_{pf} \delta \frac{d(T_{fm})}{dt} = h\xi(T_\infty - T_{fs}) - \omega h_v - \frac{k_f (T_\infty - T_{fs})}{\delta} \tag{13}$$

where h and K_f are the heat transfer coefficient and the liquid fuel thermal conductivity. The terms in right hand of equation are the heat transfer rate from gas to fuel film on the gas side, the heat transfer rate used for vaporization and the heat transfer from wall to the film respectively.

This code considers some phenomena like the Liquid Film Stripping off as Droplets at Sharp Edge as well as Valve-Seat Fuel Film Squeezing When the valve descends on to the valve seat.

3.8. Combustion models

The correlative combustion model for premixed charge spark ignited engines is based on a Wiebe function relationship widely used to describe the rate of mass burned in thermodynamic calculations. It represents quite well the experimentally observed trends of combustion heat release. When using the Wiebe correlation, the cumulative mass fraction burned as a function of crank angle is given by the following:

$$W = 1 - \exp\left[-AWI\left(\frac{\Delta\theta}{BDUR}\right)^{(w\exp+1)} \right] \quad (14)$$

where $\Delta\theta$ is crank degrees past start of combustion, BDUR, user-entered 10-90% burn duration in crank degrees, W_{exp}, user-entered Wiebe exponent and AWI, internally calculated parameter to allow BDUR to cover the range of 10-90%. When using the Wiebe model, the combustion rate is controlled by three user-defined parameters. These are the location (in degrees) of the 50% burned point of the total heat release, the burn duration (in degrees) from 10% to 90% mass burned and the Wiebe function exponent.

4. INJECTOR MODEL

Droplet probability distribution and droplet size distribution are defined according Rosin & rambler distributions and fuel delivery diagram that determines delivery fuel mass versus injection duration is provided using experimental data of full consumption of engine in specified load as is represented in table 3. The injection parameters e.g. the nozzle geometry, mean diameter of droplets (SMD) and spray cone angle are to be specified since they are required for the fuel evaporation and impingement model. Also, the injection velocity (deduced from the injection pressure) and start of injection in crank angle is used in the model. These parameters are defined by testing the injector using PDA technique in various fuel pressures and temperatures are shown in table 2 & 3.

Table 3: Delivered fuel mass from injector versus injection pulse width in fuel pressure 300 Kpa

pulse width (ms)	fuel consumption (kg/hr)	Mass (mgr)
4.52	2.41	7.72
6.21	3.43	10.99
7.89	4.43	14.19
8.64	4.9	15.7
10.27	5.9	18.91
10.98	6.3	20.19
13.169	7.6	24.358
14.74	8.638	27.68

5. CALIBRATING THE MODEL

Accuracy of model was verified using experimental results of engine testing and values of some engine parameters like volumetric efficiency, in cylinder pressure diagram, Torque, manifold pressure, air to fuel ratio and exhaust gas temperature in full load condition and velocity range of 2600 rpm to 6000 rpm were used. For this means, computerize modeling values of mentioned parameters were compared to experimental data of engine testing. Figure 6 presents values of volumetric efficiency and torque for both the model and engine testing and shows the good agreement between the model and the real engine operation.

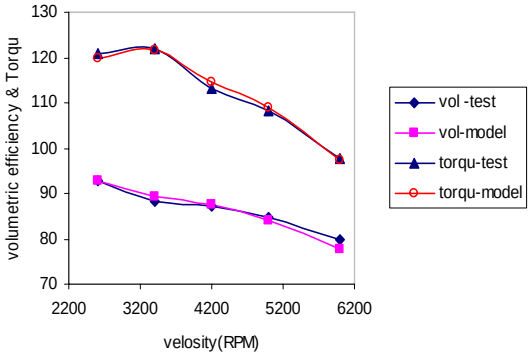

Fig. 6: Comparing modeling values of volumetric efficiency and torque with warm testing data

6. RESULTS AND DISCUSSIONS

The multi component fuel is assumed to be $C_{7.3}H_{13.9}$. The main thermo physical properties of fuel are listed in Table 4. The geometric and other boundary conditions used in the model are summarized in Table 5. The geometric and other parameters used in the model are based on a XU7JP-L3 model 4-cylinder engine.

The duration of the droplet injection time, which is supposed to keep a lean mixture with λ=1.02 in 2600 rpm. Incoming air flow, is a function of the manifold pressure, charge temperature and engine speed.

Table 4: Thermo physical properties

Stoichiometric A/F	14.57
Surface tension (N/m)	$20*10^{-3}$
Vapor pressure (kpa)	50
Viscosity (N.s/m^2)	$450*10^{-6}$
Density (kg/m^3)	750
Latent Heat (kJ/kg)	340
Boiling temperature (k)	340
Formula	$C_{7.3}H_{13.9}$

Table 5: Property of intake charge to port in full load condition

Velocity (rpm)	Initial gas velocity	Intake charge temperature	Intake manifold pressure	Intake wall temperature
2600	50 (m/s)	304 (k)	0.862 (bar)	360 (k)
6000	113 (m/s)	299 (k)	0.806 (bar)	460 (k)

For the engine operating conditions, the duration of the droplet injection time and intake-exhaust valve lift diagram is shown in Figure 7. The end time of injection in full load condition is supposed to be in 320 ATDC and injection pulse width is 230 deg. and 550 deg. for 2600 rpm and 6000 rpm respectively.

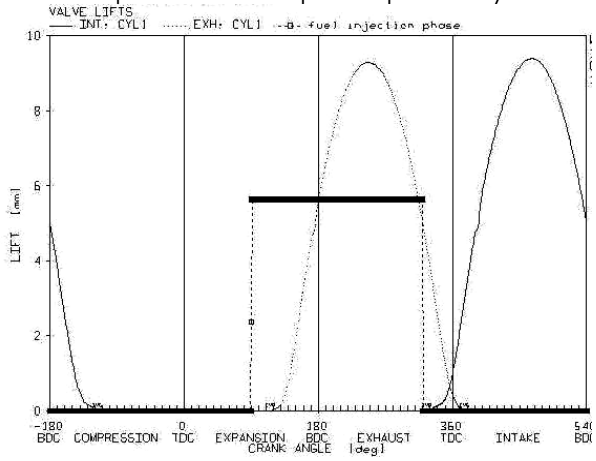

Fig. 7: The duration of the droplet injection time and intake-exhaust valve lift

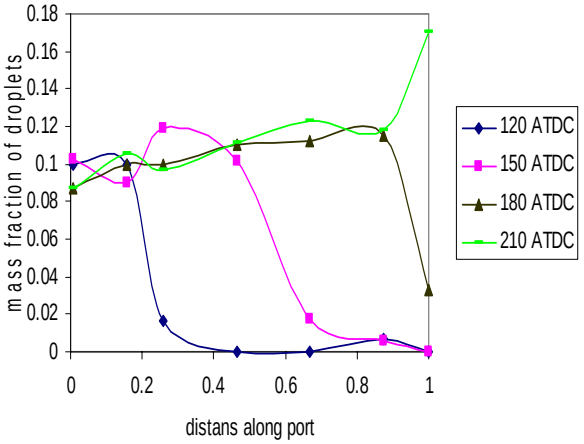

Fig. 8: The droplet stream locations after fuel injection at different times

Figure 8 shows the droplet stream locations in the first event after fuel injection at different times. It represents that the droplets stream already reaches to the intake valve in 150 deg. ATDC or 4 ms after injection start time. In following, mass fraction of droplets increases in the end of intake port and extends toward upper hand of the port.

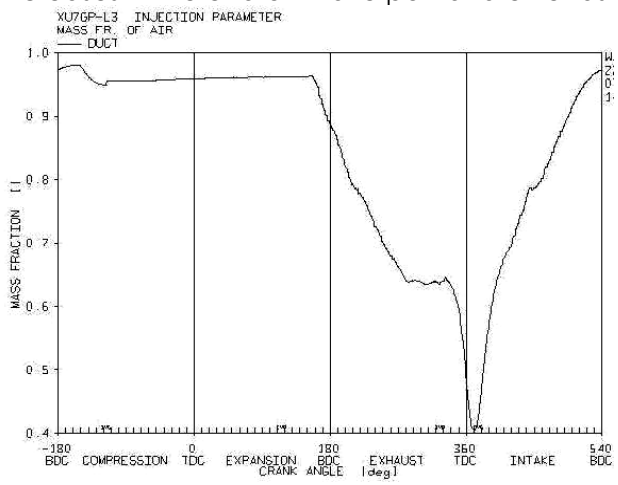

Fig. 9: Mass fraction of air in one complete engine cycle in 2600 rpm

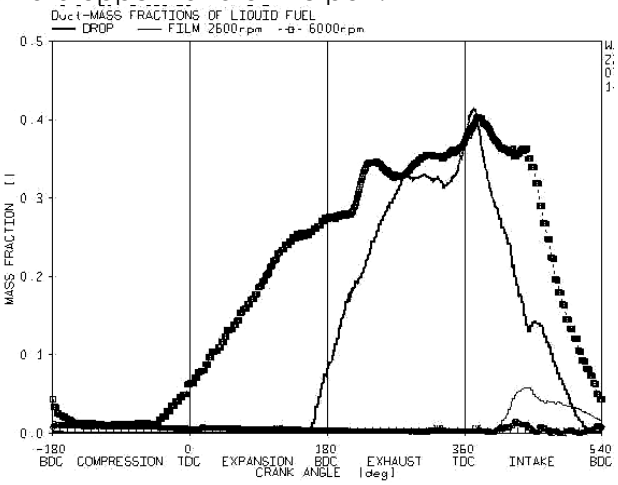

Fig. 10: Mass fraction of liquid phase (droplet & liquid film) at the end of intake port in 2600 rpm (simple line) and 6000 rpm (thick marked line)

Figure 9 shows the air mass fraction in a complete engine cycle which includes intake, compression, expansion and exhaust strokes. According to this Figure mass fraction of air remains constant while the intake valve is close and it decreases once the fuel is injected to the port. It should be noticed that injection of fuel occurs in a close valve condition. Once

the intake valve opens, mass fraction of air decreases sharply in cause of back flow of hot gases to the port from cylinder.

The mass fraction of liquid phase consisted of droplet and fuel film at the end of intake port is shown in Figure 10 for both 2600 and 6000 rpm conditions. The diagram for 6000 rpm is shown with thick marked lines. Since the intake charge flow push the fuel droplets downward the port, the liquid fuel film is formed in end of the port after that the intake valve is opened and it reaches to the cylinder 4.5 ms after intake valve opening. As it is observed, at 2600 rpm, all of fuel droplets pass the intake port and enter to the cylinder during the first half period of intake stroke. Also all of the droplets enter to the cylinder before closing the intake valve at 6000 rpm. It is an important strategy in designing the injector flow rate and injection timing.

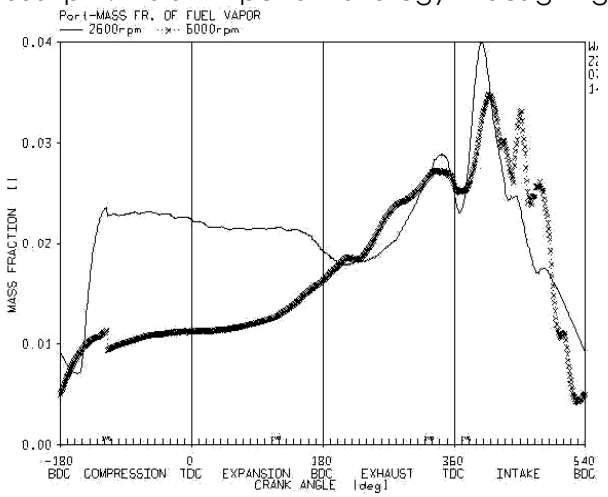

Fig. 11: Mass fraction of fuel vapor in the end of intake

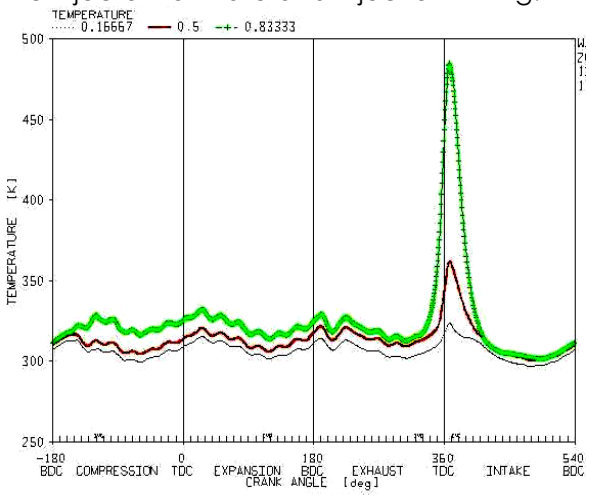

Fig. 12: Density profile of gas mixture along the port through a cycle

Figure 11 shows the mass fraction of fuel vapor in the end of intake port during a complete cycle in 2600 and 6000 rpm. As it is observed at 2600 rpm, there is some residue fuel vapor in the intake port remained from the previous cycle before fuel injection. As the fuel is being delivered, the mass fraction of fuel vapor starts to in increases and this is due to vaporization of fuel droplets. Sudden drop of diagram after opening the intake valve represent the backflow to the port. This flow is hot enough and helps the fuel droplets and fuel film in vicinity of intake valve to vaporize. As a result, the amount of fuel vapor increases suddenly and reaches to maximum amount in the beginning of intake stroke and in continue it decreases after entering all vapor to cylinder. The backflow to the port before closing the valve cause a sudden jump in amount of vapor in the port. The amount of backflow reduces with increasing the engine velocity and as it is shown in Figure 11, at 6000 rpm the backflow has a little amount compared with 2600 rpm. The higher wall temperature at 6000 rpm, the more amount of fuel vaporization from the wall surface, but because the needed time for vaporization at 6000 rpm is less than as what it is for 2600 rpm therefore the amount of vapor does not have considerable increase at 6000 rpm.

The mixture temperature significantly affects the volumetric efficiency and engine performance with changing fuel and air mixture density and amount of air which enter to the cylinder. The fuel and air mixture temperature through a cycle is shown in Figure 12 on three places along the port which marked with coefficients 0.16, 0.5 and 0.8 of the total length of port. Because of the hot gas backflow to the port, the mixture temperature suddenly increases. The effect of backflow in the intake stork is more considerable at the end zone of the port. The mixture temperature increases as it is closing to the end zone of the intake port. It accurse because of the high wall temperature and the effect of hot gas backflow to the port at the end zone of the intake port. The higher amount of evaporation through fuel injection from droplets and fuel film in the first and middle part of intake port is another reason that reduces the mixture temperature in first zone of intake port. The mixture density diagram has a reverse manner rather than temperature profile.

7. THE EFFECT OF FUEL TEMPERATURE

As the fuel temperature increases, the fuel vapor pressure on the droplets and fuel film surface increases. According eq.13 vapor generation rate of fuel is directly related to the saturated fuel pressure; therefore the fuel temperature increases the rate of droplets and liquid film vaporization via convection and diffusion.

$$x_{fs} = \frac{p_{sat}(T_s)}{p_{\infty}} \tag{13}$$

In this equation x_{fs} and p_{sat} are the mass fraction of fuel vapor and saturate vapor pressure of fuel respectively. This effect can be seen in figure 13 in which the mass fraction of fuel vapor is shown in the end of intake port in different fuel temperatures. Vaporization occurs on the surface of fuel droplet just the fuel is injected in the port and requires amount of heat for vaporization is gained from droplets and air. If the fuel droplets temperature is more than air temperature, the required heat for droplets vaporization is gained from droplets and their temperature reduce suddenly below than air temperature before droplets reach to the port surfaces. In this condition the fuel film temperature is less than the condition that fuel temperature was less than air temperature and the difference between temperature of hot moving air and cold fuel film in port increases. Therefore as a result of much heat transfer from air to fuel film, the air temperature reduces more than the first condition and in other word an increase in fuel temperature to specific point, cause the mixture temperature in port to reduces. In the other hand the mixture temperature influences on density and mass flow rate of mixture in the port and mixture density variation cause a change in the amount of mixture that enters to the cylinder, So the volumetric efficiency varies.

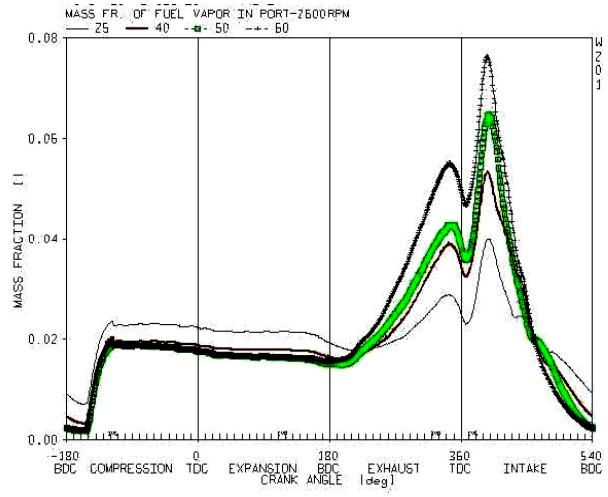

Fig. 13: The mass fraction profile of fuel vapor in the end of intake port in different fuel temperature

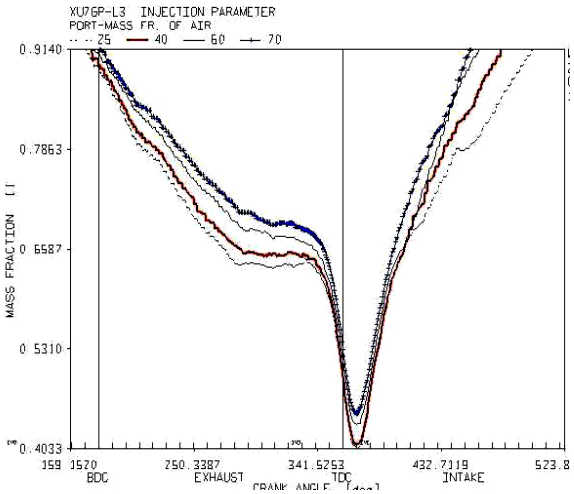

Fig. 14: The mass fraction profile of air in the end of intake port in different fuel temperature in exhaust and intake stroke

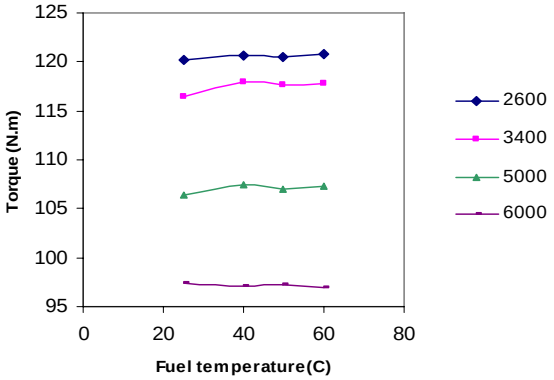

Fig. 15: Variation of brake torque with fuel temperature increasing in different velocity

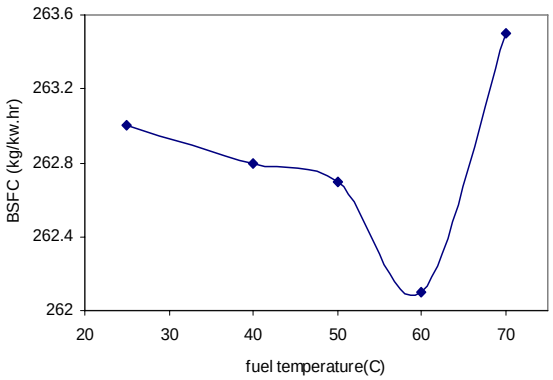

Fig. 16: Profile of Brake specific fuel consumption in different fuel temperature for 2600 rpm and full load

Figure 14 shows the mass fraction profile of the air in air and fuel mixture that pass the end of intake port in the exhaust and intake stroke in different fuel temperature. The amount of air which enters into the cylinder increase with an increase in fuel temperature to 60°c, and decrease with more increase in fuel temperature. In this condition volumetric efficiency in 2600 rev/min and full load has a maximum value in 60C. According figure 15 the maximum value of volumetric efficiency in full load condition and in 2600, 3400, 5000 and 6000 rev/min are 60, 45, 40 and 25C respectively. In other word the efficient fuel temperature decreases with an increase in engine velocity. Figure 16 shows the brake mean specific fuel consumption profile of engine in different fuel temperatures in full load condition and 2600 rpm. According this figure, the specific fuel consumption has a minimum value in fuel temperature of 60C.

8. THE EFFECT OF FUEL INJECTION PRESSURE

As the fuel pressure increases in the upper hand of injector, both jet velocity and spray con angle increases and as a result makes the diameter of droplets much smaller so a better atomization is achieved. Figure 17 shows the effect of injection pressure on spray cone angle.

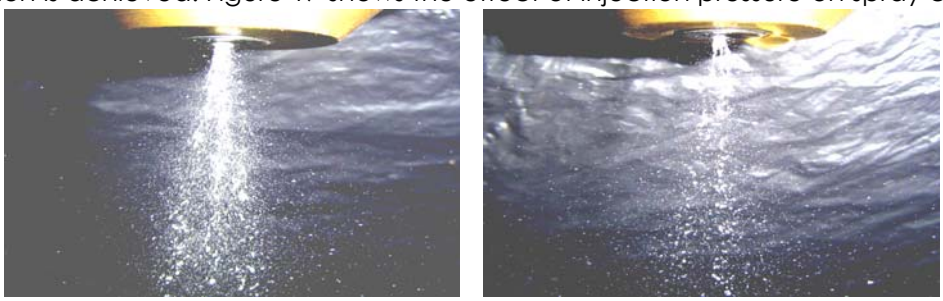

Fig. 17: The effect of injection pressure on spray cone angle (Right; 2 bar, Left: 4 bar)

The fuel injection pulse width in engine should be reduced because of the injection pressure and mass flow rate increase. So considering a specific injection end time, the fuel should be injected in the port later with increasing injection pressure that has below results:

1. Increasing vaporization rate in case of relative velocity increase of fuel injection.
2. Reduction in droplets means diameter and increase of droplets surface contact that makes much vaporization rate.
3. Increasing the spray cone angle that provides wither spray angle and much fuel wetted surface in the intake port.
4. Reducing the in hand time for fuel vaporization in the port and cylinder because of thinner injection pulse width.

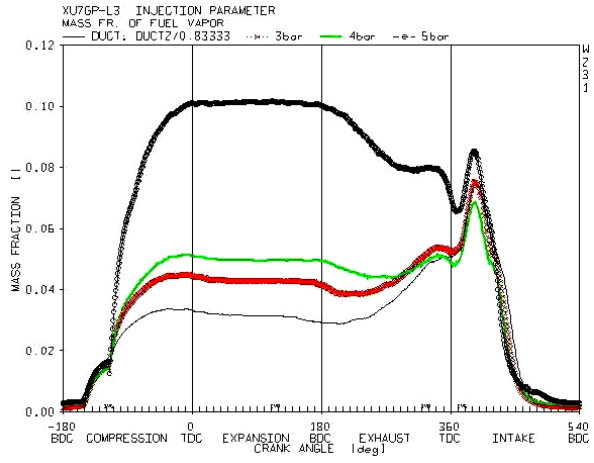

Fig.18: The mass fraction profile of fuel vapor in the end of intake port in different fuel pressures

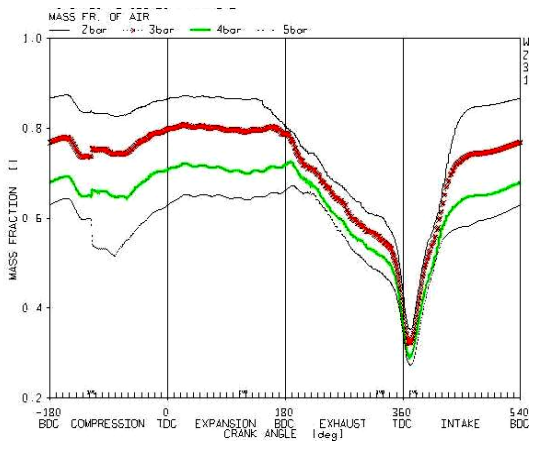

Fig. 19: The mass fraction profile of air in the end of intake port in different fuel pressure in a cycle

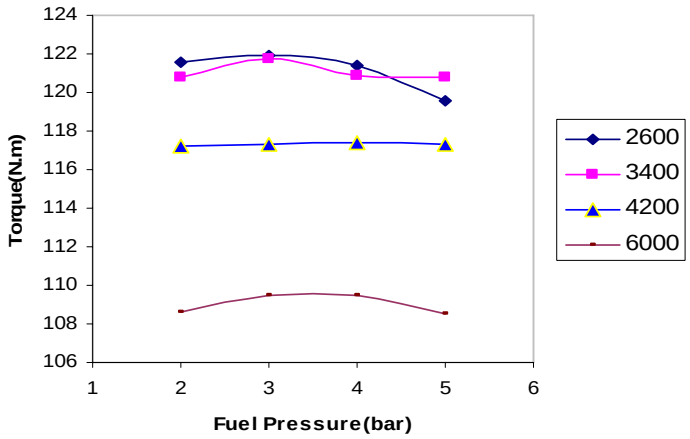

Fig. 20: Variation of brake torque with fuel pressure increasing in different engine velocity

Figure 18 shows the effect of injection pressure on mass fraction of fuel vapor in the intake port. As far as the intake port geometry and engine modeling are concerned an increase in fuel pressure lets much fuel vapor form in the intake port upon intake valve opening.

Figure 19 shows the mass fraction profile of air in the end of intake port in different fuel injection pressures. According this figure, an increase in fuel pressure causes a reduction in the mass fraction and as a result it seems that volumetric efficiency reduces. In figure 20 the effect of fuel pressure on brake torque in full load condition and in range of 2600 and 6000 rpm is shown. According this figure, engine brake torque has a maximum value in fuel pressure 3 bar and as a result in this condition the brake specific fuel consumption has a minimum value.

9. CONCLUSIONS

According to the present investigation, it was found that the injector produces a finer spray with a wide spray angle in higher fuel pressures and temperatures which refine fuel-air mixture characteristics in intake port. A specific fuel temperature also produces optimum condition for fuel consumption and performance and this fuel temperature reduces with engine velocity increase.

REFERENCES

[1] Zhao, F. Q., Yoo, J. H., Lai, M.C. The Spray Characteristics of Dual-Stream Port Fuel Injectors for Applications to 4-Valve Gasoline Engines, SAE Technical Paper, No. 952487, 1995.

[2] Zhao, F.-Q., Lai, M.-C. and Harrington, D. L. The Spray Characteristics of Automotive Port Fuel Injection - A Critical Review, SAE Technical Paper, No. 950506, 1995.

[3] W. Min Ren, H. Sayar. "Influence of Nozzle Geometry on Spray Atomization and Shape for Port Fuel Injector ", SAE Technical Paper, No. 01-0608, 2001.

[4] Lai, M.-C., Zhao, F.-Q. "The Structure of Port Injector in Gasoline Engines," Proceedings of Advanced Spray Combustion (ISASC), Hiroshima, Japan, July 6-8, 1994, pp.79-89.

[5] SAE Recommended Practice, "Gasoline Fuel Injector ", SAE J1832 NOV89, P: 99-115.

[6] S.K.Chen, A.Lefebvre. "Influence of Ambient Air Pressure on Effervescent Atomization ", AIAA Journal, 1993, pp10-15.

[7] S.D.Jackson, P.Williams. "Development of a Fuelling System to Reduce Cold-Start Hydrocarbon Emissions in an SI Engine ", SAE Technical Paper, No. 961119, 1996.

[8] Senda, J., Nishikori, T., Tsukamoto, T., and Fujimoto, H. "Atomization of Spray under Low-Pressure Field from Pintle Type Gasoline Injector," SAE Technical Paper, No. 920382, 1992.

[9] Senda, J., Yamaguchi, M., Tsukamoto, T., and Fujimoto, H. "Characteristics of Spray Injected from gasoline Injector (2nd Report, Effect of Back Pressure)," JSME Trans., Vol.58, No.553, pp.2919-2924, 1992.

[10] Chen, G., Aggarwal, s. "Unsteady Multiphase Intake Flow in a Port-injected Gasoline Engine ", SAE paper 960074, 1996.